Electronic Supplementary Material (ESI) for Chemical Communications

The enantiomers of *syn*-2,3-difluoro-4-aminobutyric acid elicit opposite responses at the $GABA_C$ receptor

*Izumi Yamamoto, Meredith J. T. Jordan, Navnath Gavande, Munikumar R. Doddareddy, Mary Chebib and Luke Hunter**

SUPPORTING INFORMATION

Contents:

(2*S*,3*S*)-2,3-Difluoro-4-aminobutyric acid hydrochloride (**2**.HCl)

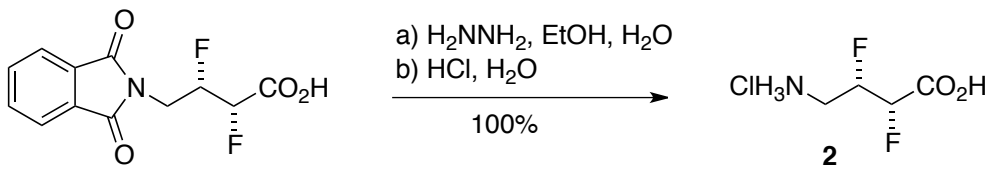

A solution of (2*S*,3*S*)-2,3-difluoro-4-phthalimidobutyric acid[1] (159 mg, 0.59 mmol) and hydrazine hydrate (57 μL, 1.2 mmol) in ethanol (12 mL) was heated at reflux overnight, then cooled and concentrated *in vacuo*. The residue was triturated in 4 M aq. HCl (4 mL) and filtered through celite. The filtrate was concentrated, then triturated in water (4 mL) and filtered again. The filtrate was concentrated to furnish the title compound as an off-white solid (106 mg, 100%); **m.p.** 178–188 °C; **[α]$_D$** +4.6 (c 0.22, H_2O); **IR** (neat) ν_{max} (cm^{-1}) 3369, 2930, 1747, 1607, 1503, 1206, 1151, 1089, 1055; **^{1}H NMR** (300 MHz, D_2O) δ 5.29 (ddddd, *J* = 46.1, 26.2, 8.8, 3.0, 1.5 Hz, 1H, β-CHF), 5.24 (ddddd, *J* = 47.5, 31.3, 1.5, 1.5, –1.5 Hz, 1H, α-CHF), 3.46 (ddddd, *J* = 17.3, 14.0, 8.8, –1.4, –0.8 Hz, 1H, γ-C<u>H</u>H), 3.45 (ddddd, *J* = 32.1, 14.0, 3.0, 1.5, –0.5 Hz, 1H, γ-CH<u>H</u>); **^{13}C {^{1}H} NMR** (75 MHz, D_2O) δ 169.9 (dd, *J* = 24.8, 3.5 Hz), 88.9 (dd, *J* = 178.5, 18.4 Hz), 88.1 (dd, *J* = 188.4, 19.6 Hz), 39.9 (dd, *J* = 21.2, 6.0 Hz); **^{19}F NMR** (282 MHz, D_2O) δ –204.1 (m, 1F, β-CHF), –206.3 (m, 1F, α-CHF); **^{19}F {^{1}H} NMR** (282 MHz, D_2O) δ –204.1 (d, *J* = 9.5 Hz, 1F, β-CHF), –206.3 (d, *J* = 9.5 Hz, 1F, α-CHF); **HRMS** (ESI, +ve) $C_4H_8NO_2F_2^+$ requires *m*/*z* 140.0518, found 140.0514.

(2*R*,3*R*)-2,3-Difluoro-4-aminobutyric acid hydrochloride (**3**.HCl)

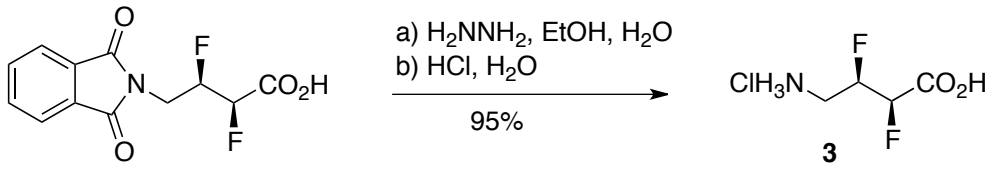

A solution of (2*R*,3*R*)-2,3-difluoro-4-phthalimidobutyric acid[1] (17.0 mg, 0.063 mmol) and hydrazine hydrate (6.1 μL, 0.12 mmol) in ethanol (1.3 mL) was heated at reflux overnight, then cooled and concentrated *in vacuo*. The residue was triturated in 4 M aq. HCl (1 mL) and filtered through celite. The filtrate was concentrated, then triturated in water (1 mL) and filtered again. The filtrate was concentrated to furnish the title compound as an off-white solid (10.6 mg, 95%); **m.p.** 185–190 °C; **[α]$_D$** –5.4 (c 0.18, H_2O); **IR** (neat) ν_{max} (cm^{-1}) 3394, 3013, 1751, 1639, 1607, 1501,

1449, 1401, 1206, 1152, 1055; **NMR** data identical to **2**; **MS** (ESI, +ve) *m*/*z* 140 ([M–Cl]$^+$, 100%); **HRMS** (ESI, +ve) $C_4H_8NO_2F_2^+$ requires *m*/*z* 140.0518, found 140.0500.

(2*R*,3*S*)-2,3-Difluoro-4-aminobutyric acid hydrochloride (**4**.HCl)

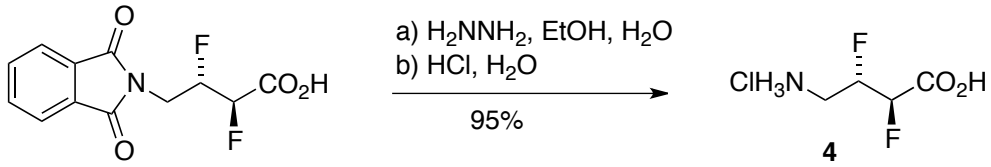

A solution of (2*R*,3*S*)-2,3-difluoro-4-phthalimidobutyric acid[1] (18.8 mg, 0.070 mmol) and hydrazine hydrate (6.8 μL, 0.14 mmol) in ethanol (1.5 mL) was heated at reflux overnight, then cooled and concentrated *in vacuo*. The residue was triturated in 4 M aq. HCl (1 mL) and filtered through celite. The filtrate was concentrated, then triturated in water (1 mL) and filtered again. The filtrate was concentrated to furnish the title compound as a moist off-white solid (11.7 mg, 95%); **[α]$_D$** –5.1 (c 0.24, H_2O); **IR** (neat) ν_{max} (cm^{-1}) 3407, 2964, 1738, 1613, 1505, 1415, 1215, 1115, 1081, 1048; **^{1}H NMR** (300 MHz, D_2O) δ 5.30 (ddddd, *J* = 47.1, 21.6, 1.9, –0.9, –1.1 Hz, 1H, α-CHF), 5.21 (ddddd, *J* = 47.8, 21.8, 9.6, 2.3, 1.9 Hz, 1H, β-CHF), 3.43 (ddddd, *J* = 14.9, 14.1, 9.6, 0.8, –0.9 Hz, 1H, γ-C<u>H</u>H), 3.30 (ddddd, *J* = 33.3, 14.1, 2.3, 1.4, –1.1 Hz, 1H, γ-CH<u>H</u>); **^{13}C {^{1}H} NMR** (100 MHz, D_2O) δ 169.7 (dd, *J* = 22.2, 9.1 Hz), 89.3 (dd, *J* = 180.0, 22.2 Hz), 88.7 (dd, *J* = 187.9, 20.9 Hz), 39.1 (dd, *J* = 21.0, 8.7 Hz); **^{19}F NMR** (282 MHz, D_2O) δ –198.1 (ddddd, *J* = 48.1, 22.2, 13.5, 2.8, 2.7 Hz, 1F), –199.1 (ddddd, *J* = 48.2, 33.7, 20.9, 14.4, 13.5 Hz, 1F); **^{19}F {^{1}H} NMR** (282 MHz, D_2O) δ –198.1 (d, *J* = 13.5 Hz, 1F), –199.1 (d, *J* = 13.5 Hz, 1F); **MS** (ESI, +ve) *m*/*z* 140 ([M–Cl]$^+$, 100%); **HRMS** (ESI, +ve) $C_4H_8NO_2F_2^+$ requires *m*/*z* 140.0518, found 140.0526.

(2*S*,3*R*)-2,3-Difluoro-4-aminobutyric acid hydrochloride (**5**.HCl)

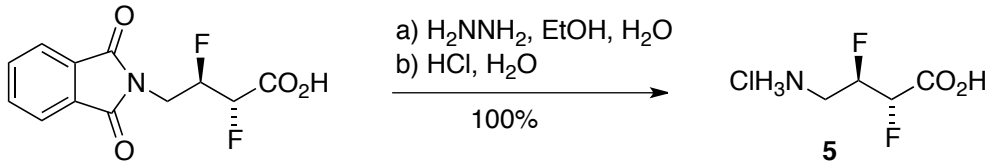

A solution of (2*S*,3*R*)-2,3-difluoro-4-phthalimidobutyric acid[1] (67 mg, 0.25 mmol) and hydrazine hydrate (24 μL, 0.50 mmol) in ethanol (5.2 mL) was heated at reflux overnight, then cooled and concentrated *in vacuo*. The residue was triturated in 4 M aq. HCl (2 mL) and filtered through celite. The filtrate was concentrated, then triturated in water (2 mL) and filtered again. The filtrate was concentrated to furnish the title compound as a moist off-white solid (44 mg, 100%); $[\alpha]_D$ +5.5 (c 0.16, H_2O); **IR** (neat) ν_{max} (cm^{-1}) 3407, 2964, 1738, 1613, 1505, 1415, 1215, 1115, 1081, 1048; **NMR** data identical to **4**; **HRMS** (ESI, +ve) $C_4H_8NO_2F_2^+$ requires *m*/*z* 140.0518, found 140.0515.

Determination of the enantiopurity of 2–5

The enantiopurity of several intermediates in the synthesis of **2**–**5** has previously been established by Mosher ester formation and chiral HPLC analysis.[1] Also, no epimeric products are observed by ^{1}H- or ^{19}F NMR when **2**–**5** are incorporated into short peptides.[1,2] This confirms that the samples of **2**–**5** used in this study have high optical purity.

^{1}H NMR (300 MHz, D_2O) of **2**

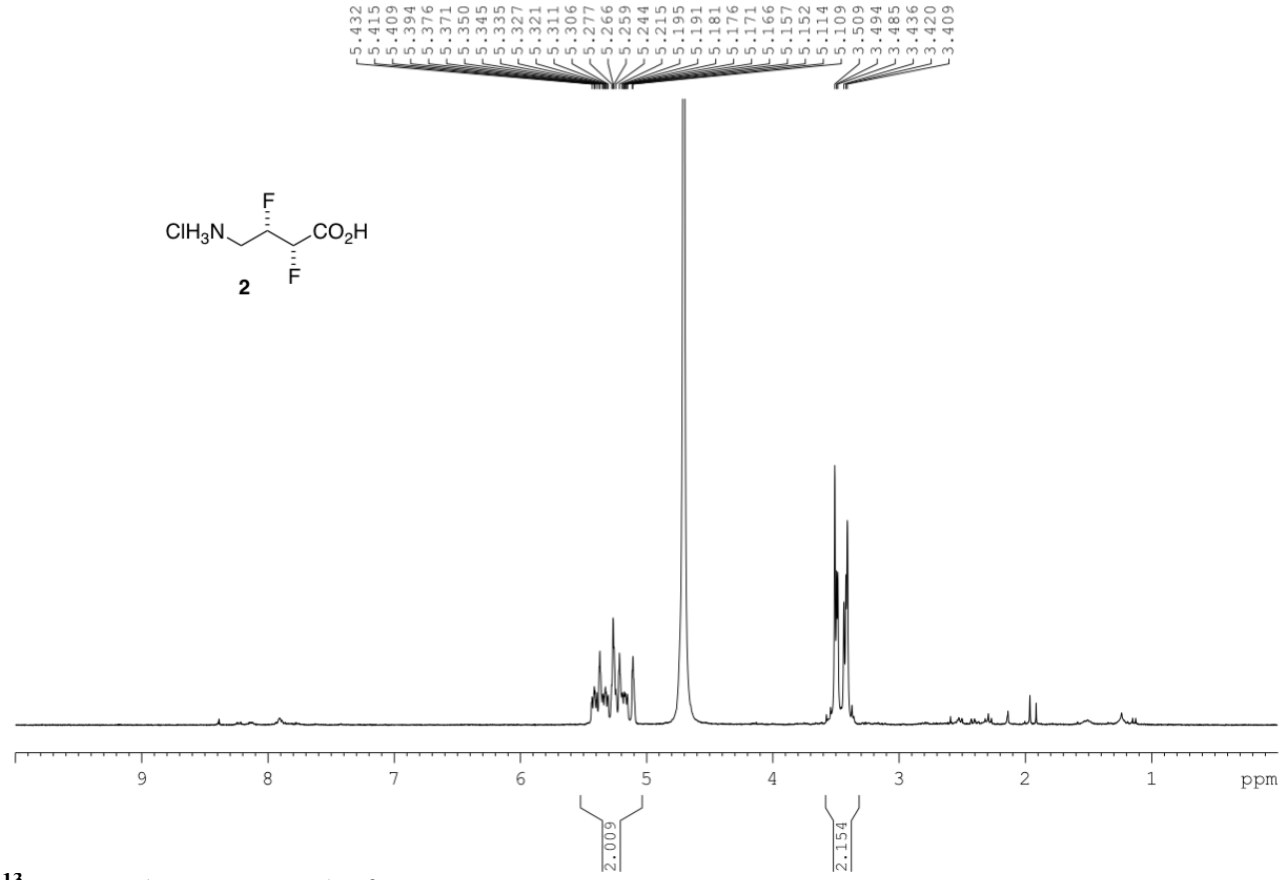

^{13}C NMR (75 MHz, D_2O) of **2**

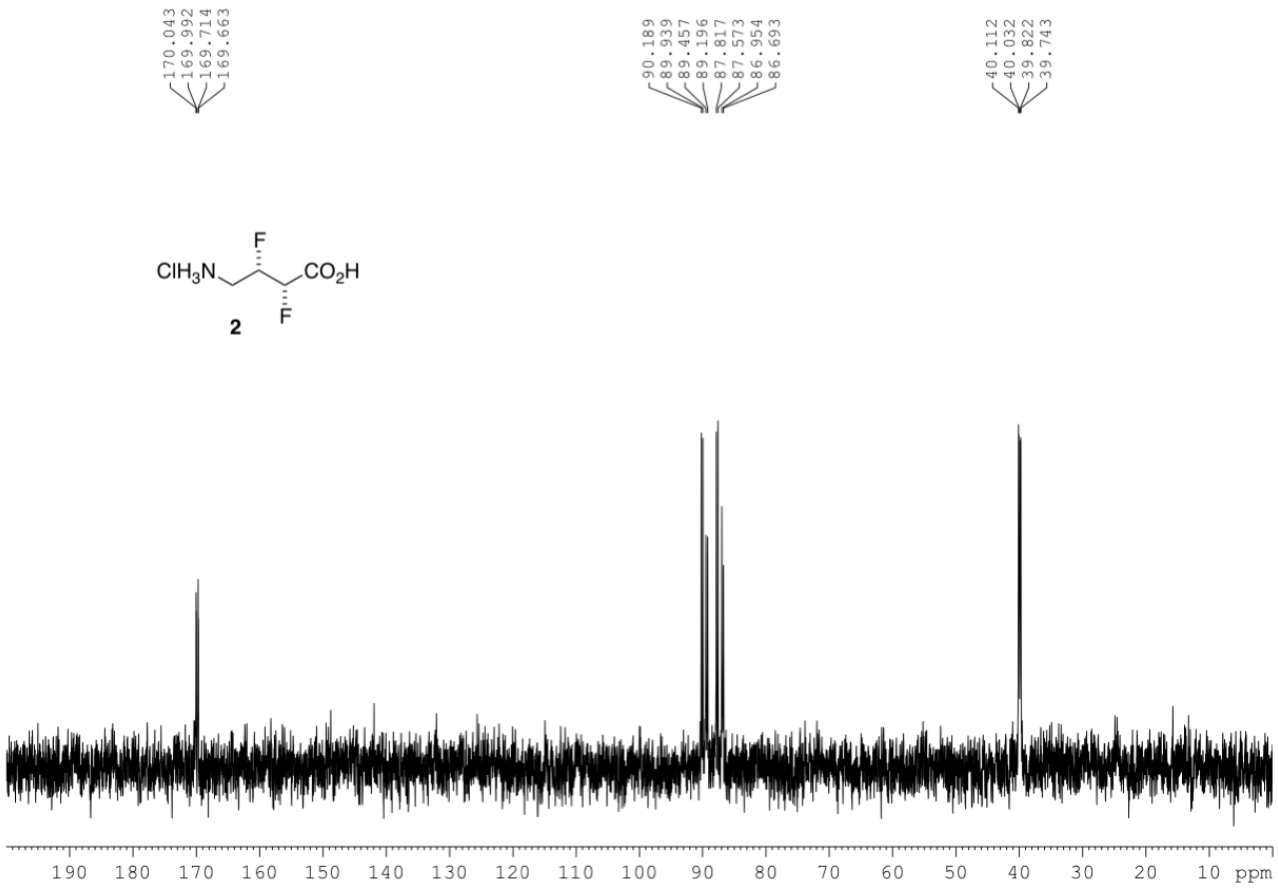

^{19}F NMR (282 MHz, D_2O) of **2**

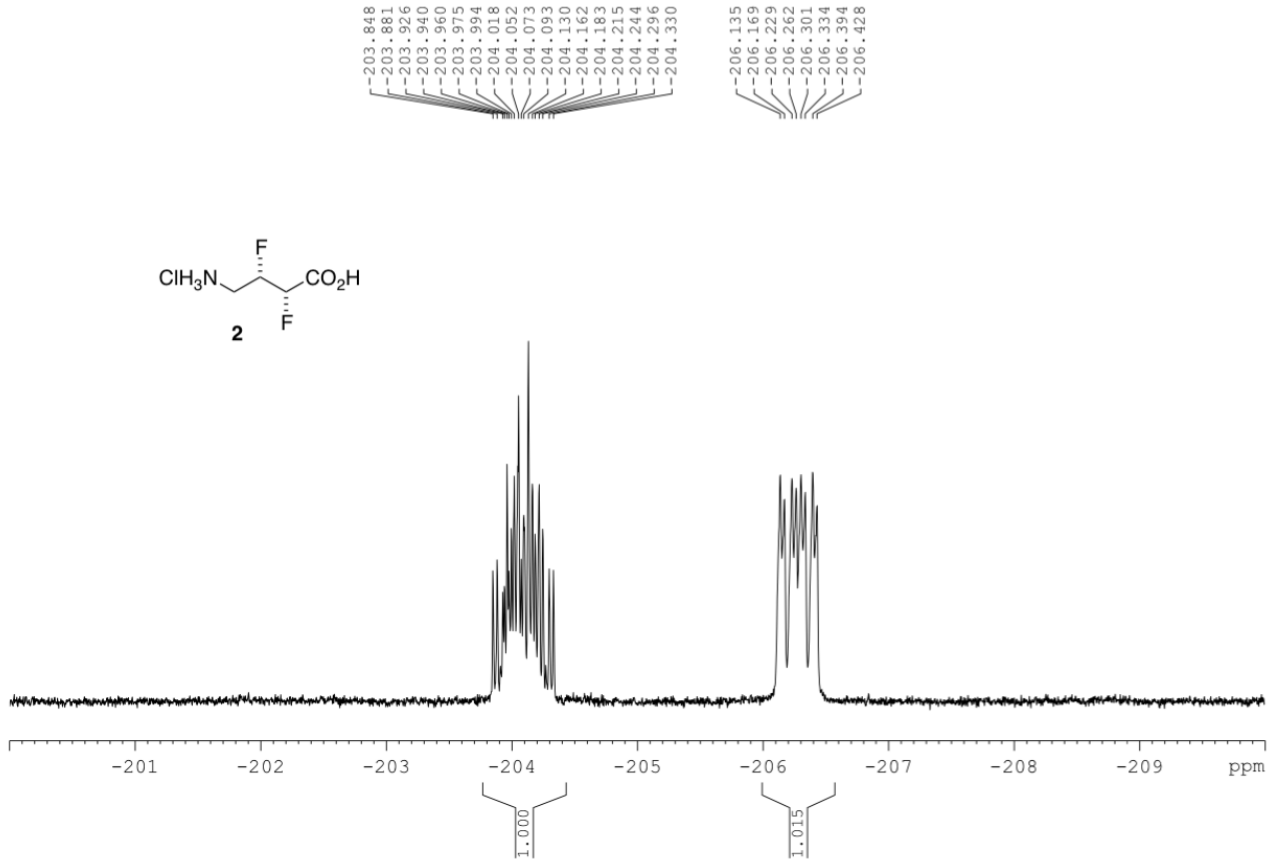

^{19}F {^{1}H} NMR (282 MHz, D_2O) of **2**

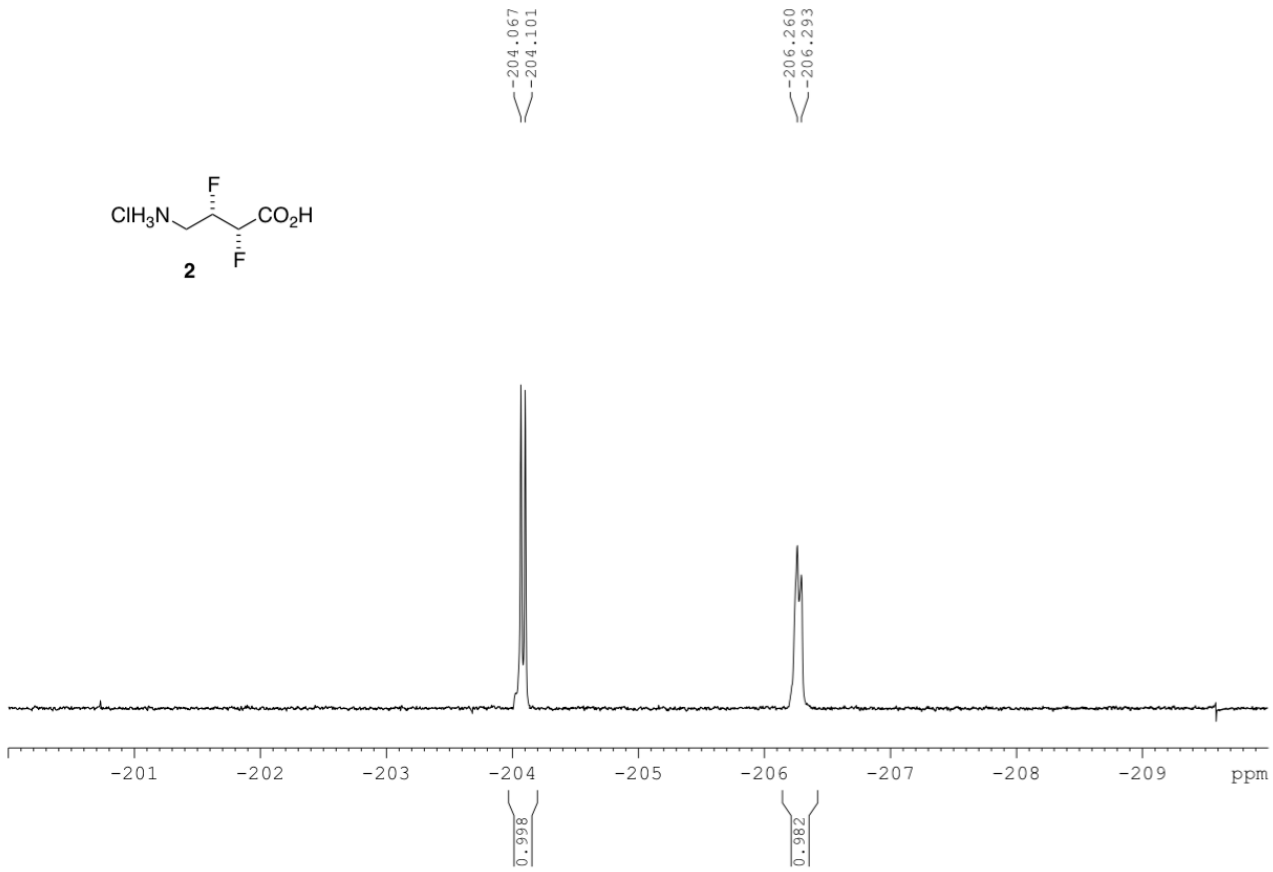

NMR simulation and measurement of coupling constants

The NMR spectra of **2** are complex, and a full analysis required software-based simulations of the experimental spectra to be performed.[3] Shown below is an overlay of the experimental (blue) and simulated (red) ^{1}H NMR spectrum of **2**.

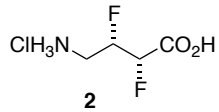

2

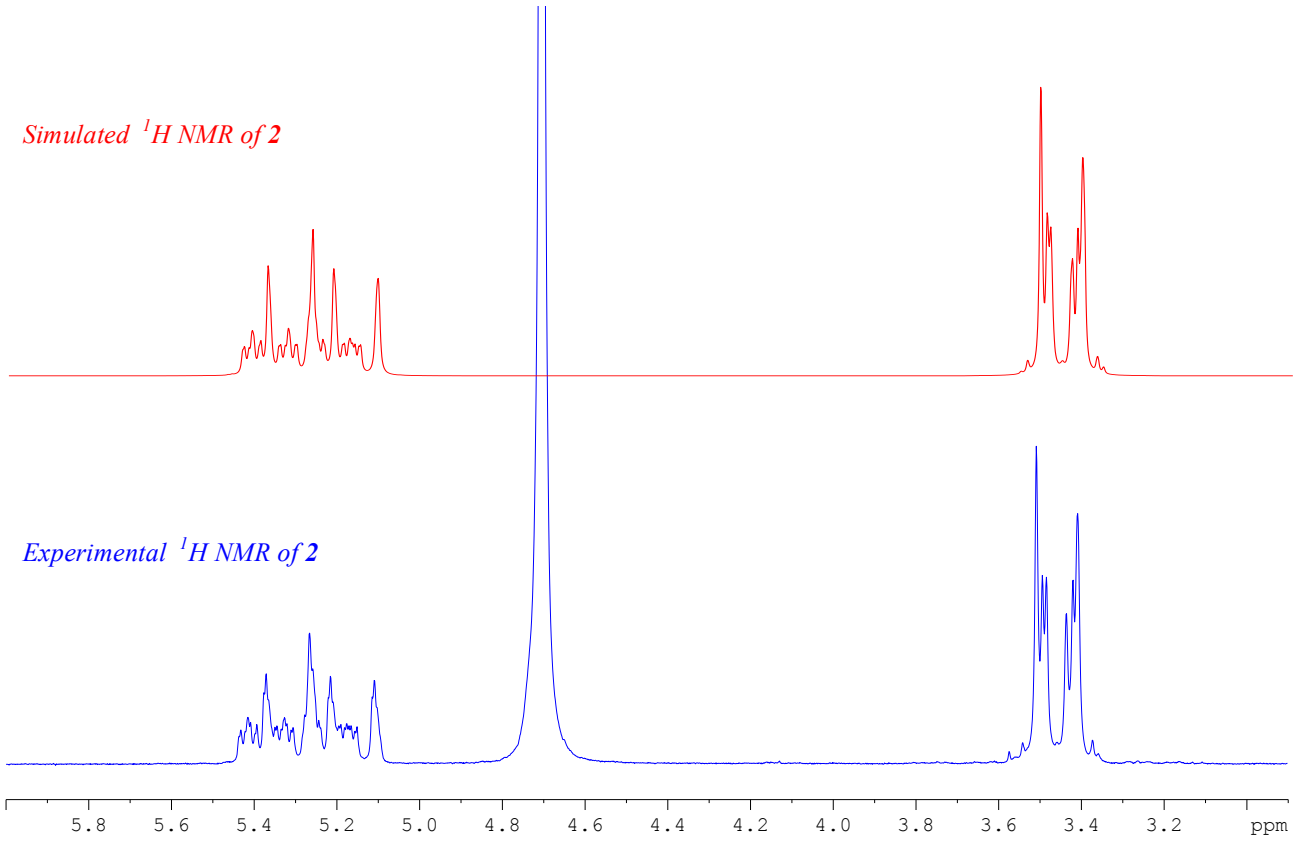

The Table below shows the coupling constants (Hz) that were used to create the simulated ^{1}H NMR spectrum of **2**.

	C2-F	C3-H	C3-F	C4-H	C4-H'
C2-H	47.5	1.5	31.3	1.5	-1.5
C2-F		26.2	9.5	-0.5	-0.8
C3-H			46.1	3.0	8.8
C3-F				32.1	17.3
C4-H					14.0

^{1}H NMR (300 MHz, D_2O) of **4**

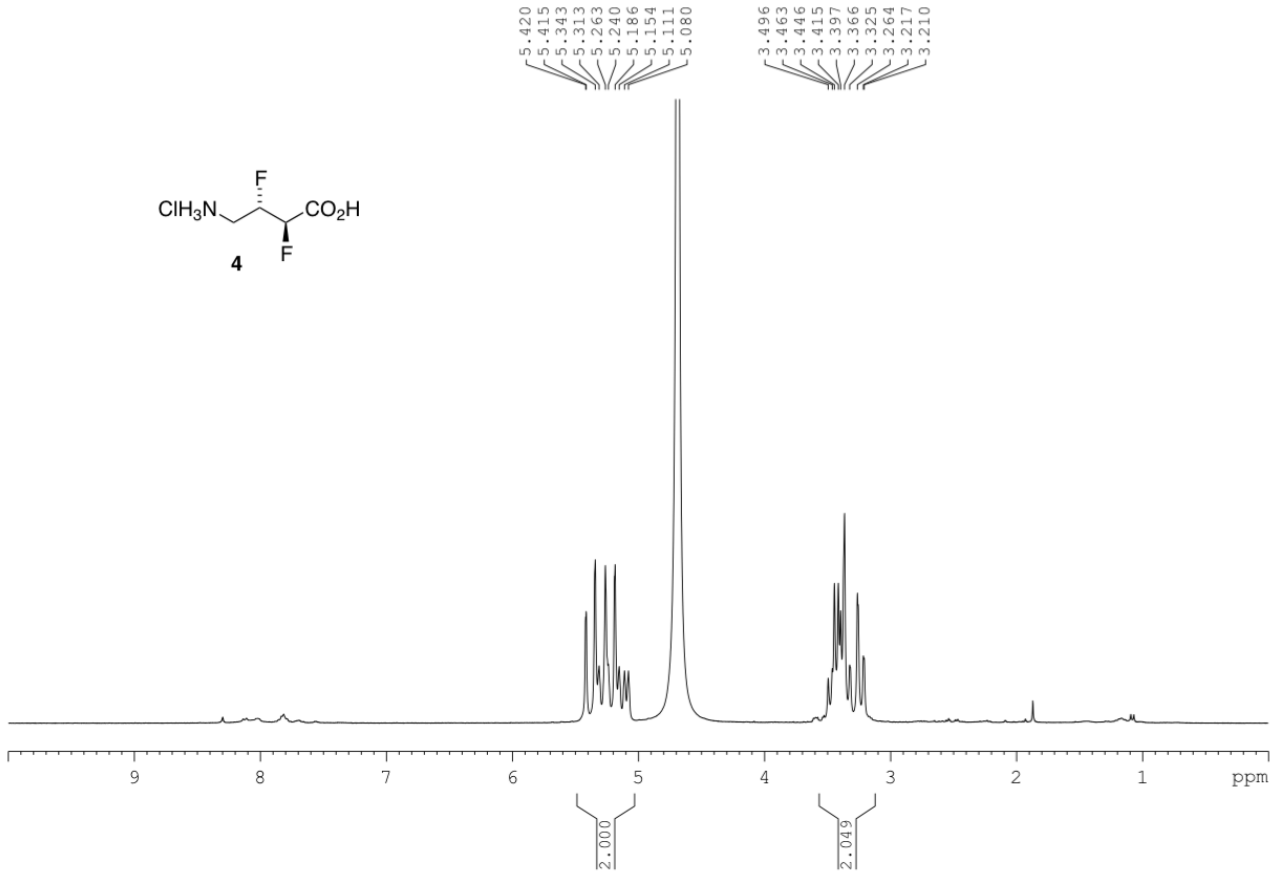

^{13}C NMR (75 MHz, D_2O, 325 K) of **4**

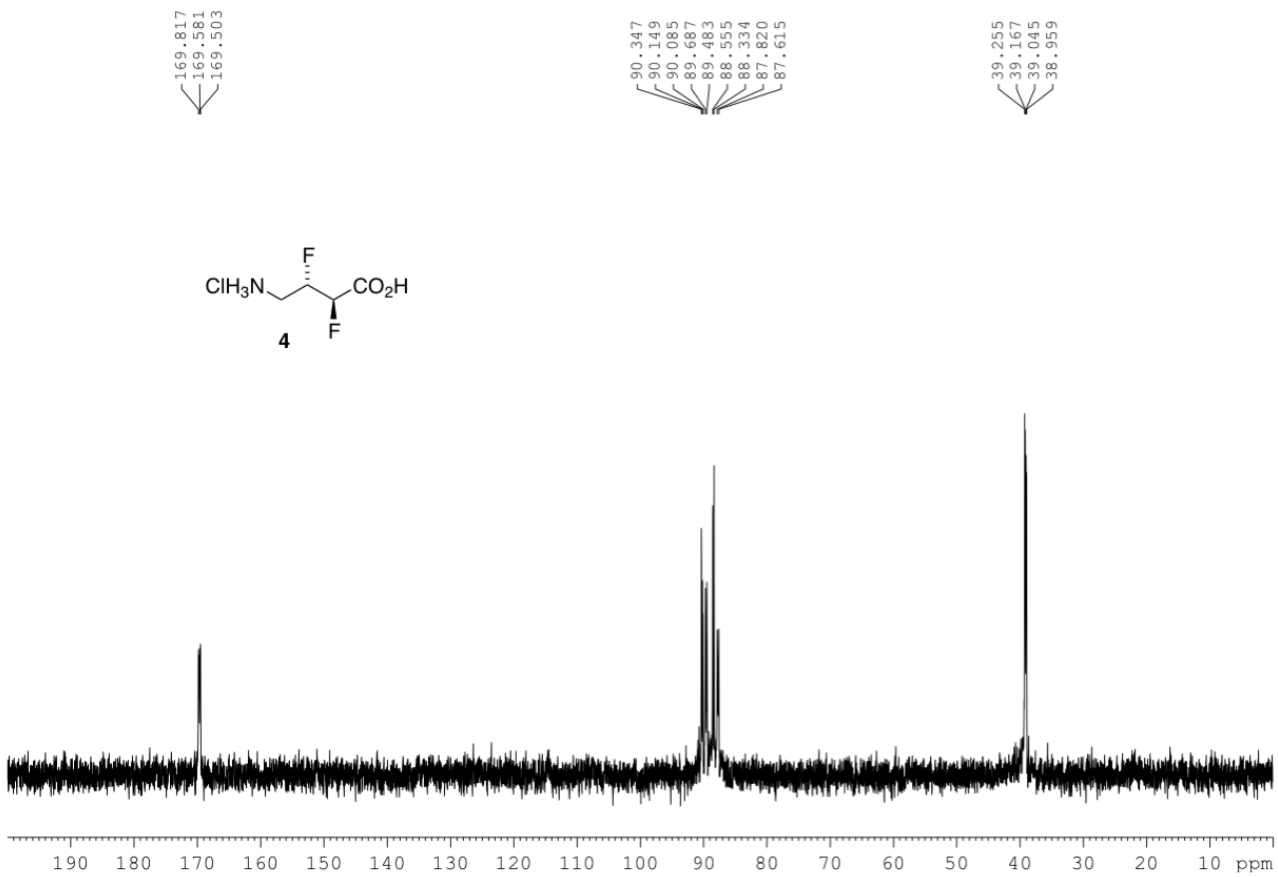

^{19}F NMR (282 MHz, D_2O) of **4**

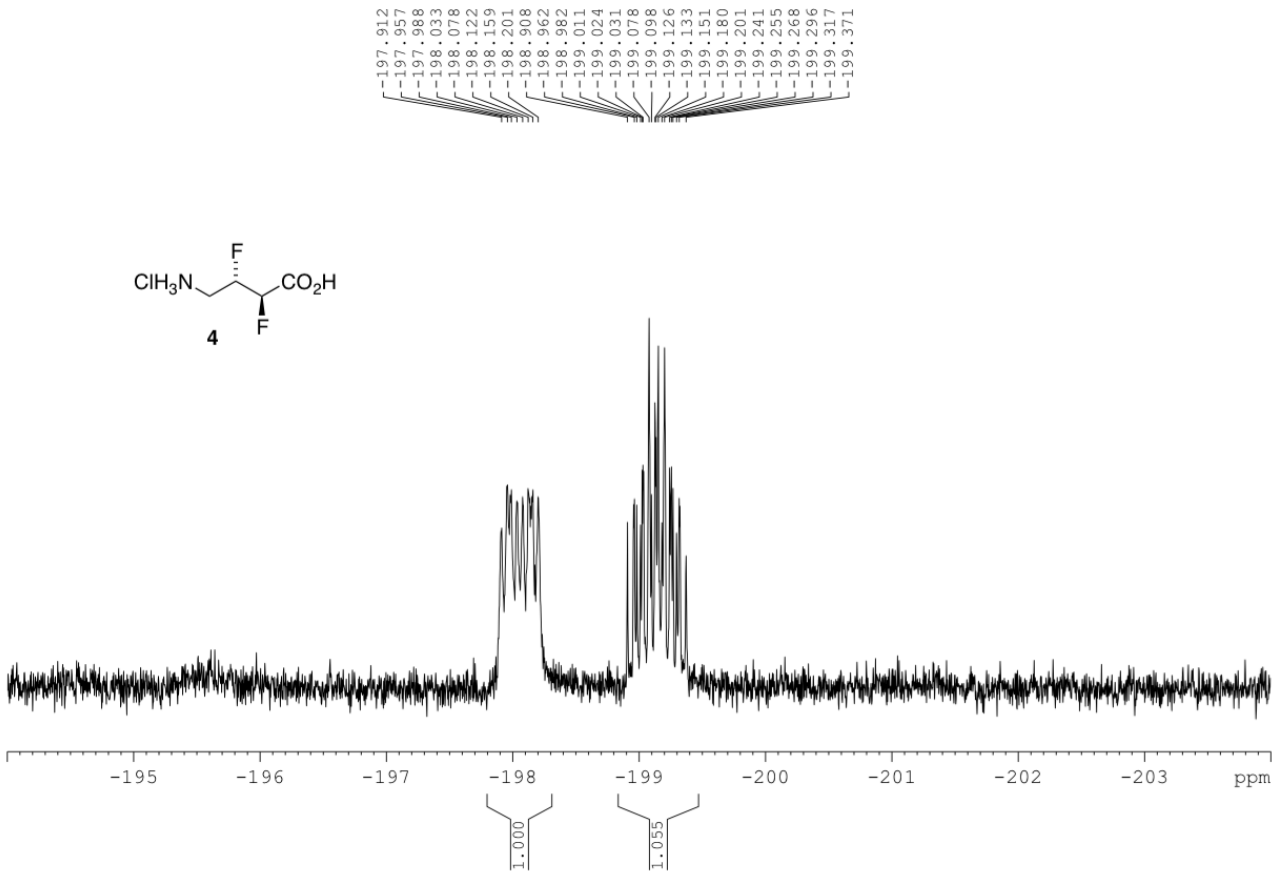

^{19}F {^{1}H} NMR (282 MHz, D_2O) of **4**

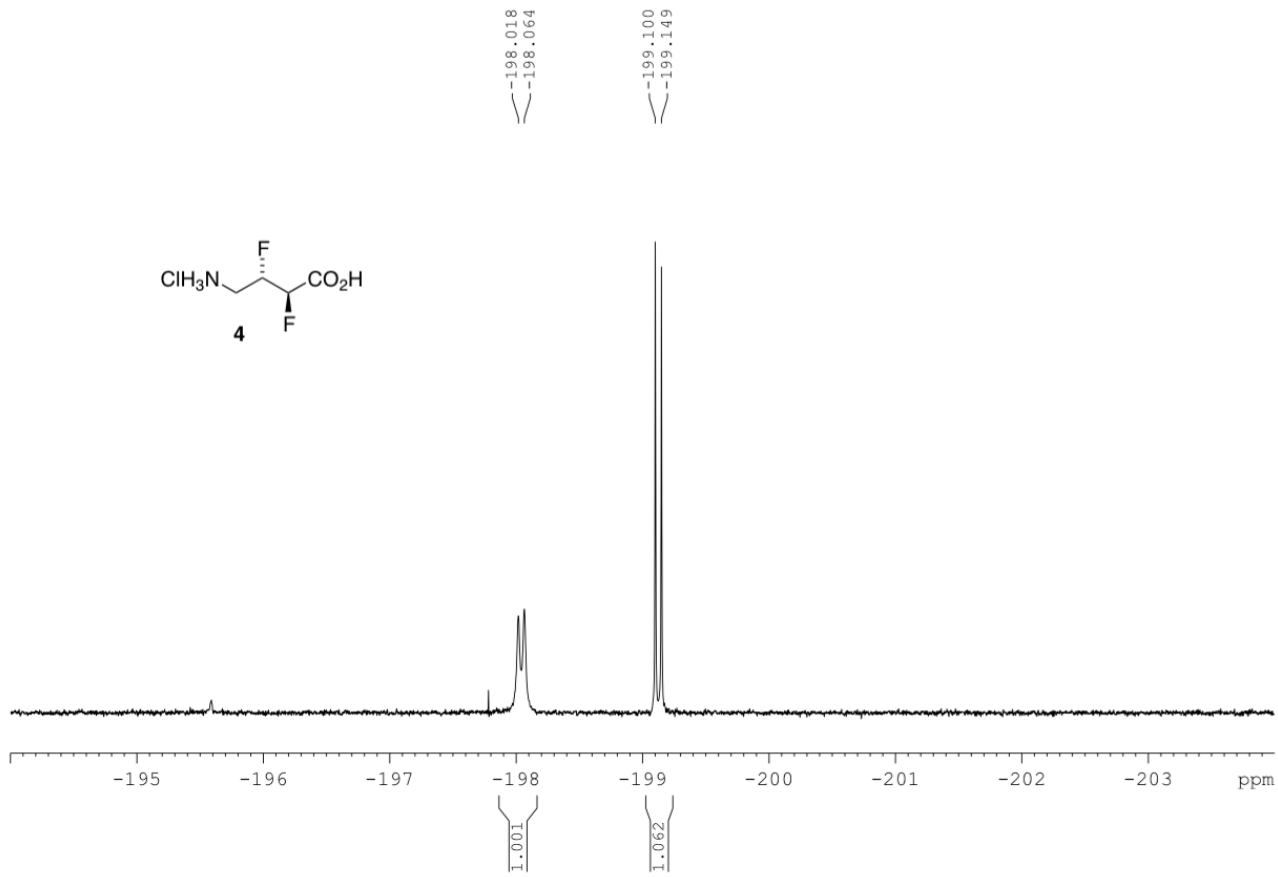

NMR simulation and measurement of coupling constants

The NMR spectra of **4** are complex, and full analyses required software-based simulations of the experimental spectra to be performed.[3] Shown below is an overlay of the experimental (blue) and simulated (red) ^{1}H NMR spectrum of **4**.

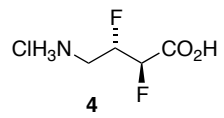

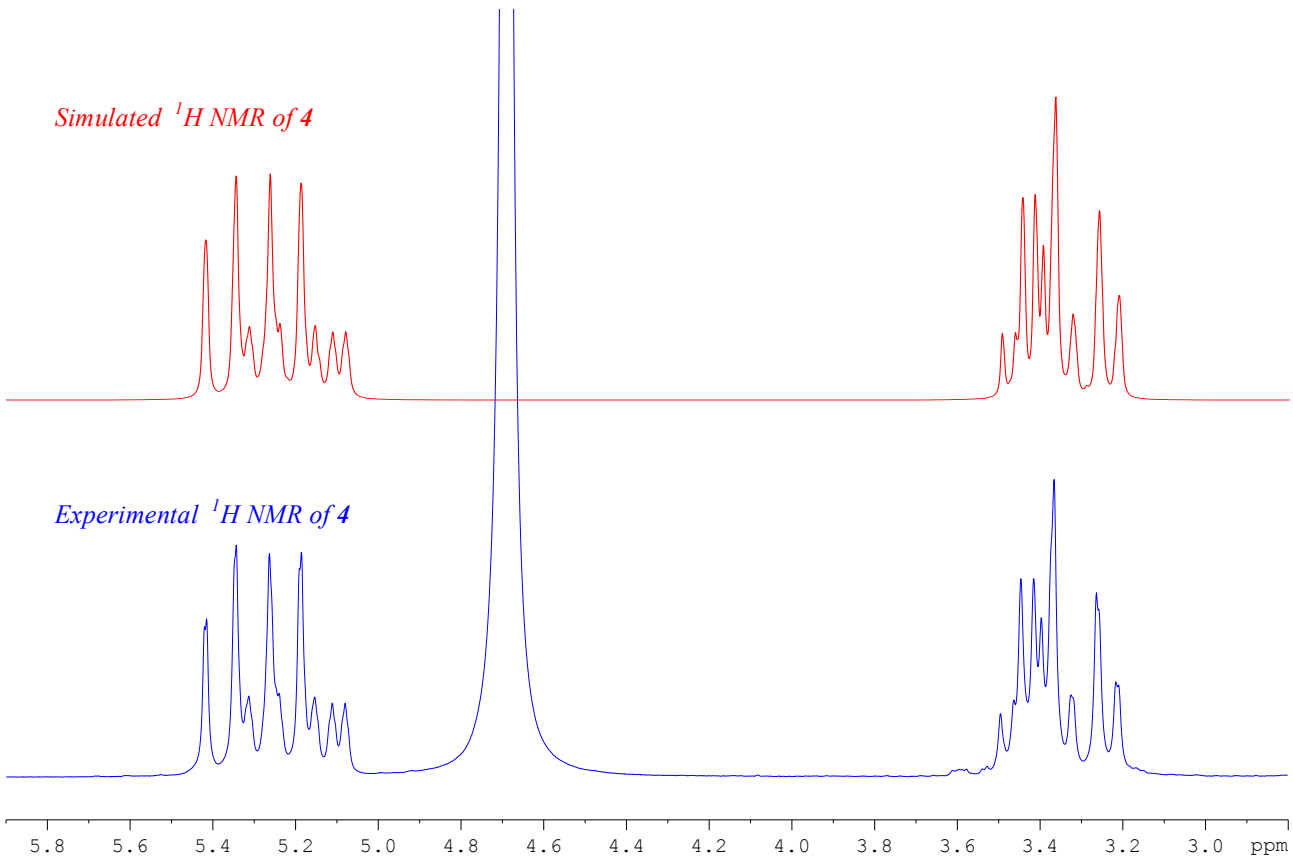

The Table below shows the coupling constants (Hz) that were used to create the simulated ^{1}H NMR spectrum of **4**.

	C2-F	C3-H	C3-F	C4-H	C4-H'
C2-H	47.1	1.9	21.6	-0.9	-1.1
C2-F		21.8	13.5	0.8	1.4
C3-H			47.8	9.6	2.3
C3-F				14.9	33.3
C4-H					14.1

Computational details

Identification of lowest energy conformers

All calculations were performed using the Gaussian09 program package,[4] with an ultrafine integration grid, on computing facilities at the Australian National Computational Infrastructure Facility (NCI). Gas-phase structures of **2**/**3** and **4**/**5** were optimised using the B3LYP hybrid density functional[5,6] and the 6-31+G(d) basis set.[7–9] The minimum energy conformers of **2**/**3** and **4**/**5** were obtained by systematic geometry optimization, giving a set of twelve local minima for **2**/**3** and eleven local minima for **4**/**5**. The nature of all local minima were confirmed by vibrational frequency analysis. Structures incorporating an intramolecular hydrogen bond were dismissed as unrealistic in an aqueous environment, leaving a refined set of six local minima for **2**/**3** and eight local minima for **4**/**5**. The relative energies in water of these conformers were then calculated using the SMD continuum solvation method of Marenich, Cramer and Truhlar,[10] and the results are shown in the Tables below.

	Conformer of **2**	Relative energy (kJ/mol) in water		Conformer of **3**	Relative energy (kJ/mol) in water
2a	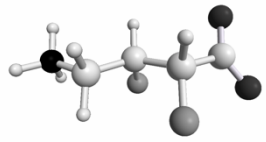	0.0	**3a**	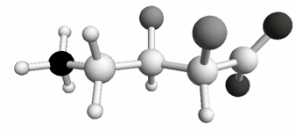	0.0
2b	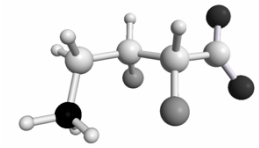	2.4	**3b**	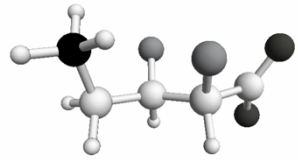	2.4
2c	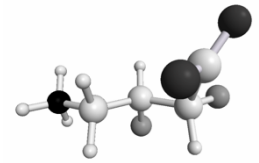	5.1	**3c**	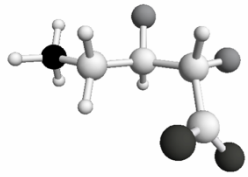	5.1

2d	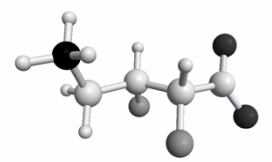	8.0	**3d**	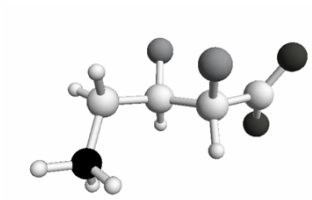	8.0
2e	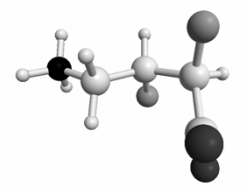	11.0	**3e**	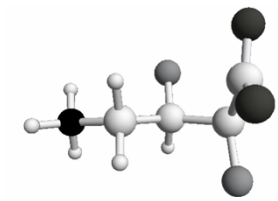	11.0
2f	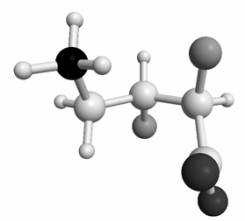	17.9	**3f**	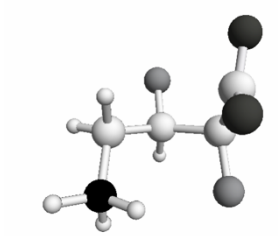	17.9

	Conformer of **4**	Relative energy (kJ/mol) in water		Conformer of **5**	Relative energy (kJ/mol) in water
4a	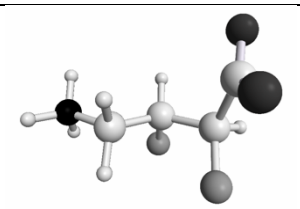	0.0	**5a**	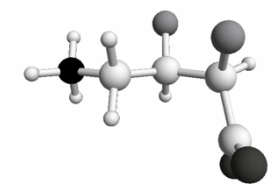	0.0
4b	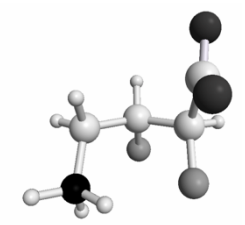	1.6	**5b**	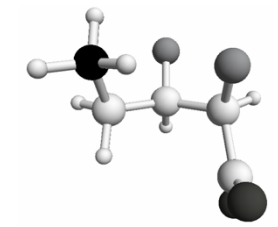	1.6
4c	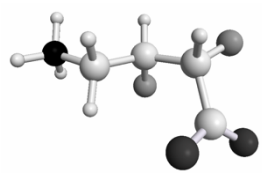	2.2	**5c**		2.2

4d	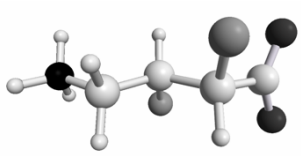	9.4	**5d**	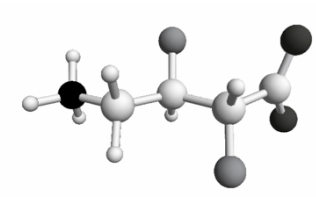	9.4
4e	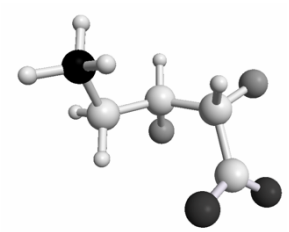	11.1	**5e**	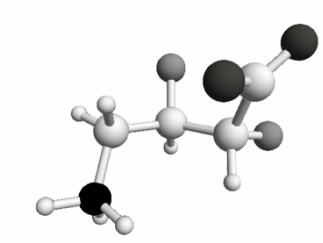	11.1
4f	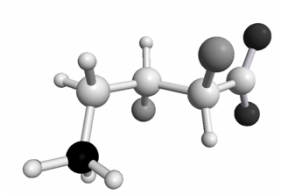	12.5	**5f**	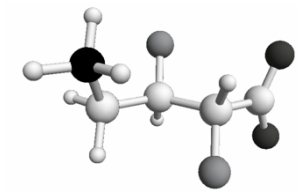	12.5
4g	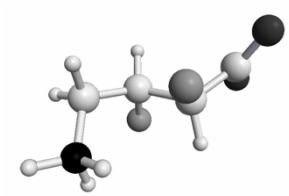	14.4	**5g**	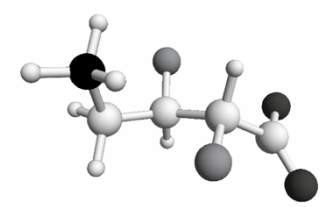	14.4
4h	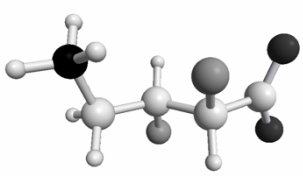	16.5	**5h**	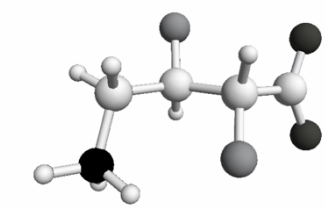	16.5

Barriers to interconversion of lowest energy conformers

The barriers to interconversion of the lowest energy conformers in aqueous solution were obtained by rotating about the N–C–C–C and/or C–C–C–C dihedral angles followed by transition state optimisation. The nature of all local minima and transition states were confirmed by vibrational frequency analysis. The results are shown in the Figures below. The maximum barrier to interconversion between **2a** and **2b** is 18.7 kJ/mol, while the maximum barrier to interconversion between **4a**, **4b** and **4c** is 15.4 kJ/mol. These barriers should be readily surmountable by a population of molecules at physiological temperature.

Interconversion between **2a** and **2b**:

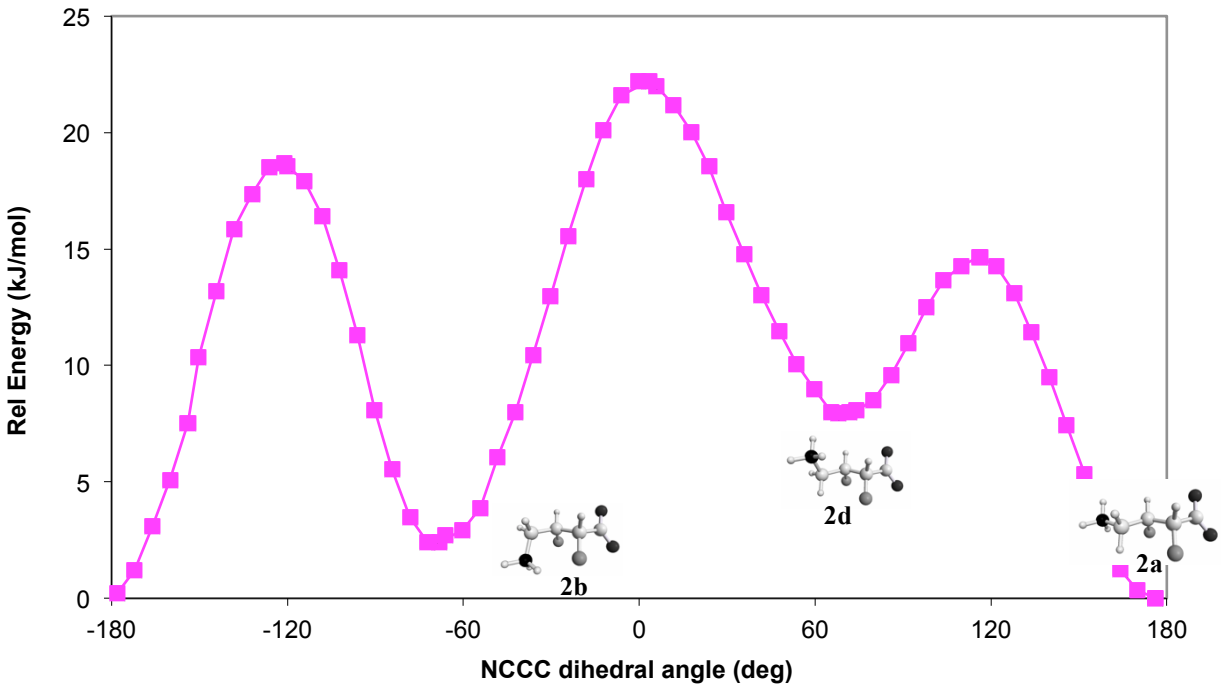

Interconversion between **4a** and **4b**:

[Note that **4b** occupies a broad shallow well, which possibly reduces the accuracy of the NMR coupling constant calculations (vide infra)]

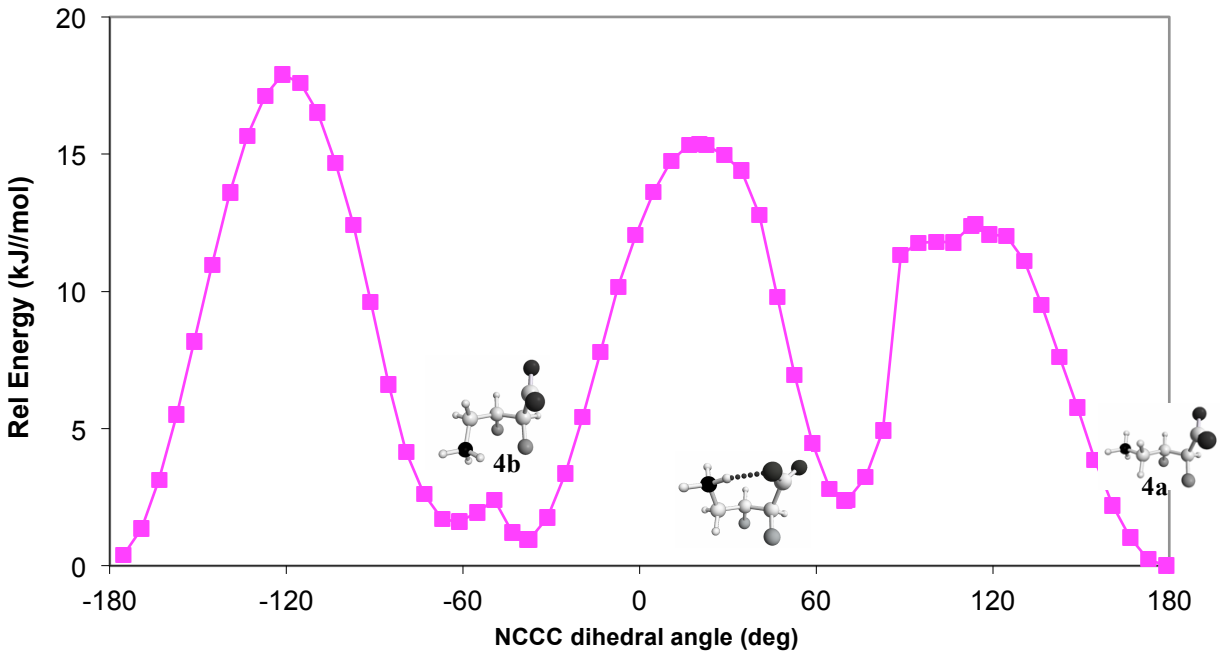

Interconversion between **4a** and **4c**:

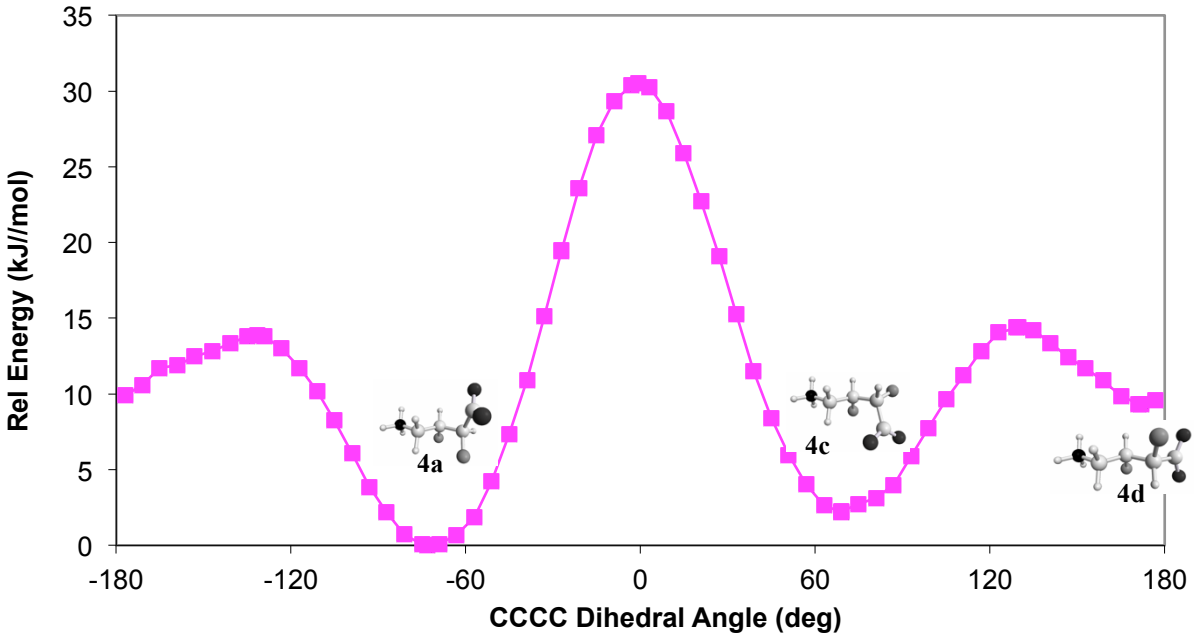

Calculated NMR coupling constants

NMR spin-spin coupling constants were calculated for **2a**, **2b**, **4a**, **4b** and **4c** using methods that were validated and optimised in a related system.[1] Calculations were performed using the SMD continuum solvation model for water, employing the gauge-invariant atomic orbital (GIAO) method[11] with the B3LYP level of theory and the Ahlrichs qzp basis set.[12] The calculated $^3J_{HH}$ and $^3J_{HF}$ values of **2a**, **2b**, **4a**, **4b** and **4c** are shown in the Tables below alongside the experimental values for **2** and **4**.

	^3J value (Hz)		
	2a	**2b**	Experimental
C2H−C3H	1.6	2.0	1.5
C3H−C4H	1.6	5.6	3.0
C3H−C4H’	10.2	0.9	8.8
C2H−C3F	32.1	33.5	31.3
C3H−C2F	23.1	29.6	26.2
C3F−C4H	35.4	3.4	32.1
C3F−C4H’	11.6	33.0	17.3

	^3J value (Hz)			
	4a	**4b**	**4c**	Experimental
C2H−C3H	2.1	2.6	1.7	1.9
C3H−C4H	10.2	1.5	9.9	9.6
C3H−C4H'	1.7	4.4	1.3	2.3
C2H−C3F	17.1	12.9	31.5	21.6
C3H−C2F	23.4	28.0	15.8	21.8
C3F−C4H	10.8	35.9	13.9	14.9
C3F−C4H'	35.7	6.7	34.2	33.3

In order to quantitatively compare the experimental and calculated NMR coupling constants, it is necessary to obtain weighted average values across the different conformers. For compound **2**, we assumed negligible contribution from any conformers other than the two lowest-energy structures **2a** and **2b**. Having made this assumption, the Boltzmann distribution was calculated to be 72.5% **2a** and 27.5% **2b** at 300 K. When the corresponding weighted average NMR coupling constants are compared with the experimentally determined values for **2**, reasonably close agreement is obtained (see Graph below), and this reflects the accuracy of the geometry optimisation and NMR coupling constant calculations. However, there is a slight disrepancy in the calculated/experimental values for C3F−C4H, possibly reflecting small contributions from other conformers.

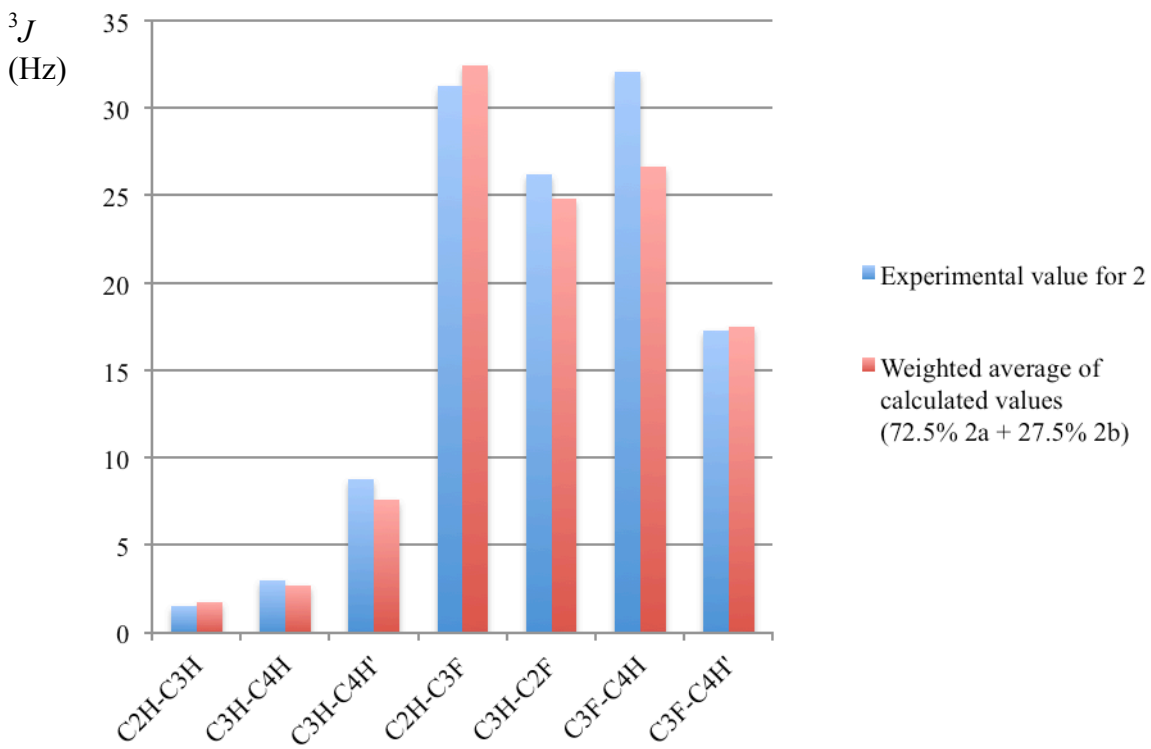

For compound **4**, we assumed negligible contribution from any conformers other than the three lowest-energy structures **4a**, **4b** and **4c**. Having made this assumption, the Boltzmann distribution was calculated to be 52% **4a**, 27% **4b** and 21% **4c** at 300 K. The corresponding weighted average NMR coupling constants are compared with the experimentally determined values for **4** in the Graph below. There is some disrepancy in the magnitude of several values, possibly reflecting small contributions from other conformers. Notably, conformer **4b** occupies a broad shallow well on the potential energy surface (vide supra) and this increases the difficulty in accurately predicting the coupling constants. Nevertheless, the overall pattern of large/small coupling constants of **4** is reasonably well predicted.

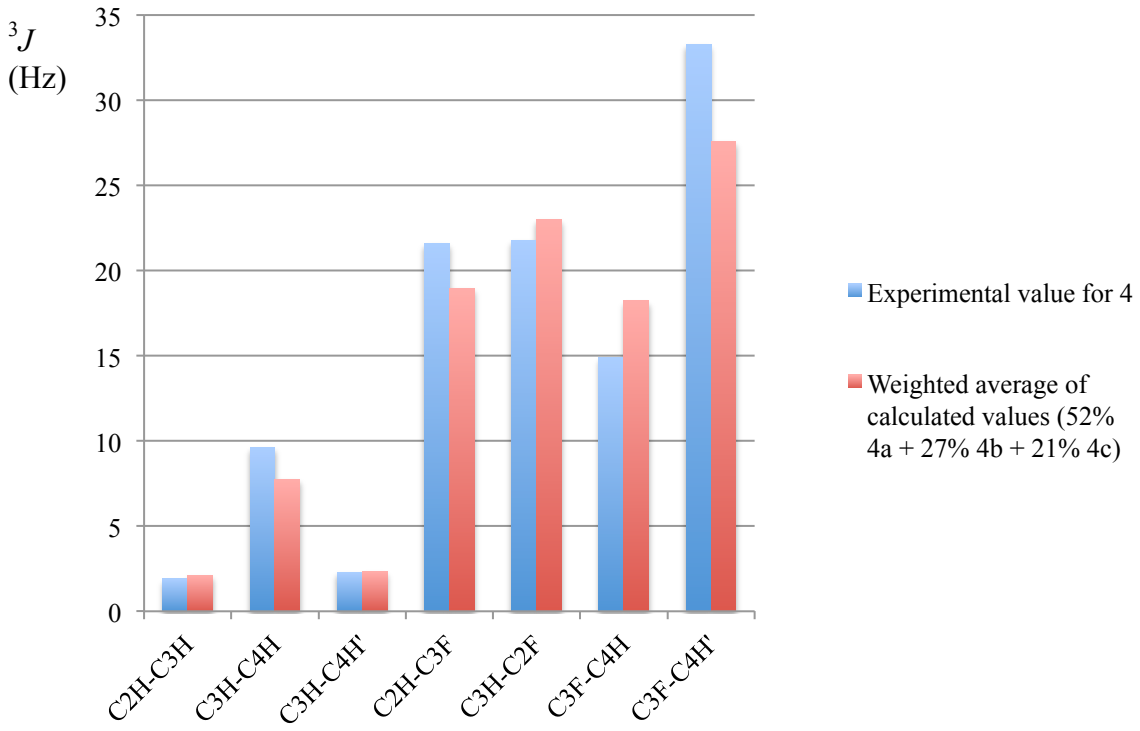

Pharmacological evaluation of 2–5 at GABA receptors

Materials

Human α1, β2, and γ2L $GABA_A$ cDNAs encapsulated into pcDM8 were gifts from Dr Paul Whiting (formerly Merck Sharpe and Dohme, Harlow, UK). Human ρ1 cDNA encapsulated in pcDNA1 was a gift from Dr George Uhl (National Institute on Drug Abuse, National Institutes of Health, Baltimore, MD). Rat GIRK4, human $GABA_{B(1b)}$ and $GABA_{B2}$ subcloned in pcDNA3.1(-), and rat GIRK1 subcloned in pBluescript were gifts from Drs Fiona Marshall and Andrew Green (formerly Glaxo Wellcome, UK). mRNAs for $GABA_{B(1b)}$, $GABA_{B2}$, GIRK1 and GIRK4 were synthesized from linearized cDNAs as previously described.[13,14] Female *Xenopus laevis* were obtained from South Africa and housed in the Edward Ford Animal House, The University of Sydney. All procedures involving animals were in accordance with the Australian Code of Practice for the Care and Use of Animals for Scientific Purposes published by the National Health and Medical Research Council of Australia (NH&MRC), and were approved by the Animal Ethics Committee of The University of Sydney.

Electrochemical assays

Pharmacological experiments were performed as previously described.[14] Whole-cell currents were measured from $GABA_A$, $GABA_B$, and $GABA_C$ receptors expressed on *Xenopus* oocytes using a two-electrode voltage clamp set-up composed of a Digidata 1200, Geneclamp 500B amplifier and pClamp 8 (Axon Instruments Inc., Foster City, CA, USA), together with a Powerlab/200 (AD Instruments, Sydney, Australia) and Chart version 5.5 program for PC.

Statistical analysis

Data are represented as the mean (±SEM) from a specified number of independent experiments. For the concentration-response curves, data points were fitted using GraphPad Prism 5. The current was normalized to the maximum concentration of agonist in the following ratio ($I/I_{GABA\ (100\ \mu M)}$) or ($I/I_{GABA\ (1\ \mu M)}$). The concentration-response curves were plotted using current ratios (Y-axis) and plotted against log of the concentration (X-axis) and fitted to the following formula:

$$I = I_{max}\,[A]^{nH}/(EC_{50}(\text{or } IC_{50})^{nH}+[A]^{nH})$$

Where I = current response, I_{max} = maximum current, n_H = Hill slope, EC_{50} = concentration that produces 50% of the response, IC_{50} = concentration that inhibits 50% of the agonist response and [A] = agonist concentration.

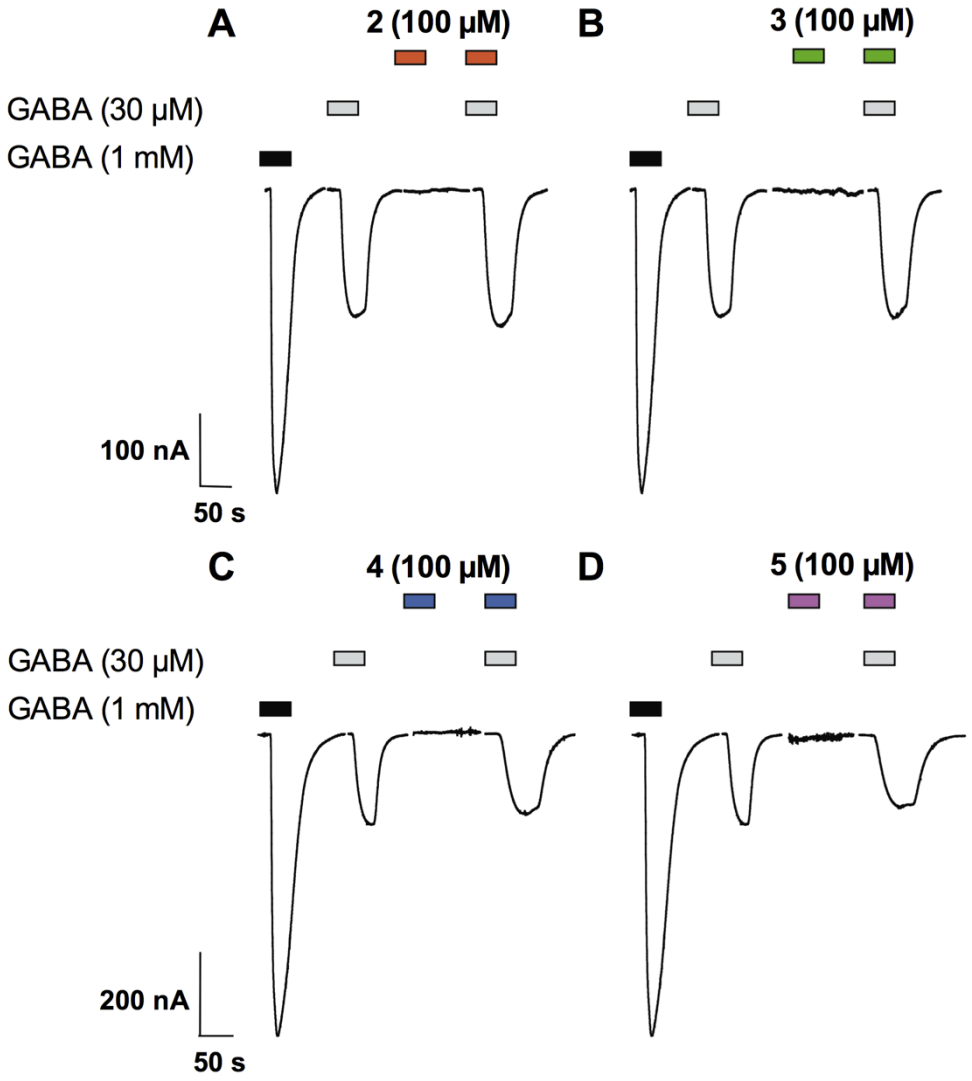

The Figure above contains sample current traces (nA vs sec) showing the effect of **2**−**5** on α1β2γ2L receptors ($GABA_A$) in *Xenopus* oocytes. **A**. **2** had no agonist effect at 100 μM (red bar), and did not inhibit the current produced by GABA (30 μM) (grey bar) **B**. **3** had no agonist effect at 100 μM (green bar), and did not inhibit the current produced by GABA (30 μM) (grey bar). **C**. **4** had no agonist effect at 100 μM (blue bar). However the current produced by GABA (30 μM) (grey bar) was inhibited by 5.3 % in the presence of **4** (100 μM) (blue bar). **D**. **5** had no agonist effect at 100 μM (pink bar). However the current produced by GABA (30 μM) (grey bar) was inhibited by 8.3 % in the presence of **5** (100 μM) (purple bar).

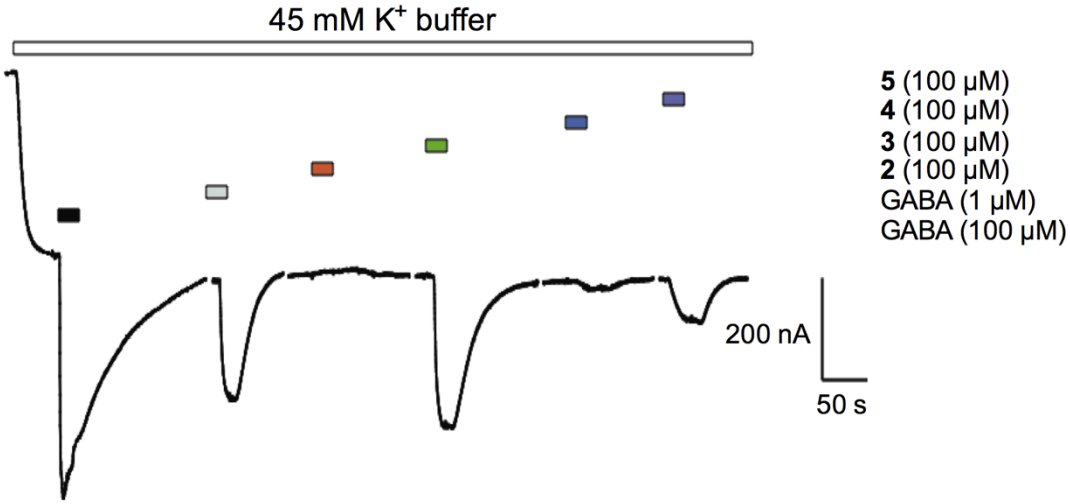

The Figure above contains a sample current trace (nA vs sec) showing the effects of **2**–**5** on human $GABA_{B(1b/2)}$ receptors coexpressed with GIRK1/4 channels in *Xenopus* oocytes. In the presence of 45 mM K^+ buffer (open bar), **2** had no effect as agonist or antagonist when tested at 100 μM (red bar). **3** (100 μM) activated the receptor by 106.4 % compared to the current produced by GABA EC_{50} (grey bar). **4** (100 μM; blue bar) and **5** (100 μM; purple bar) produced weak agonist responses alone (4.6 % and 23 %, respectively) without inhibiting the response produced by GABA (1 μM).

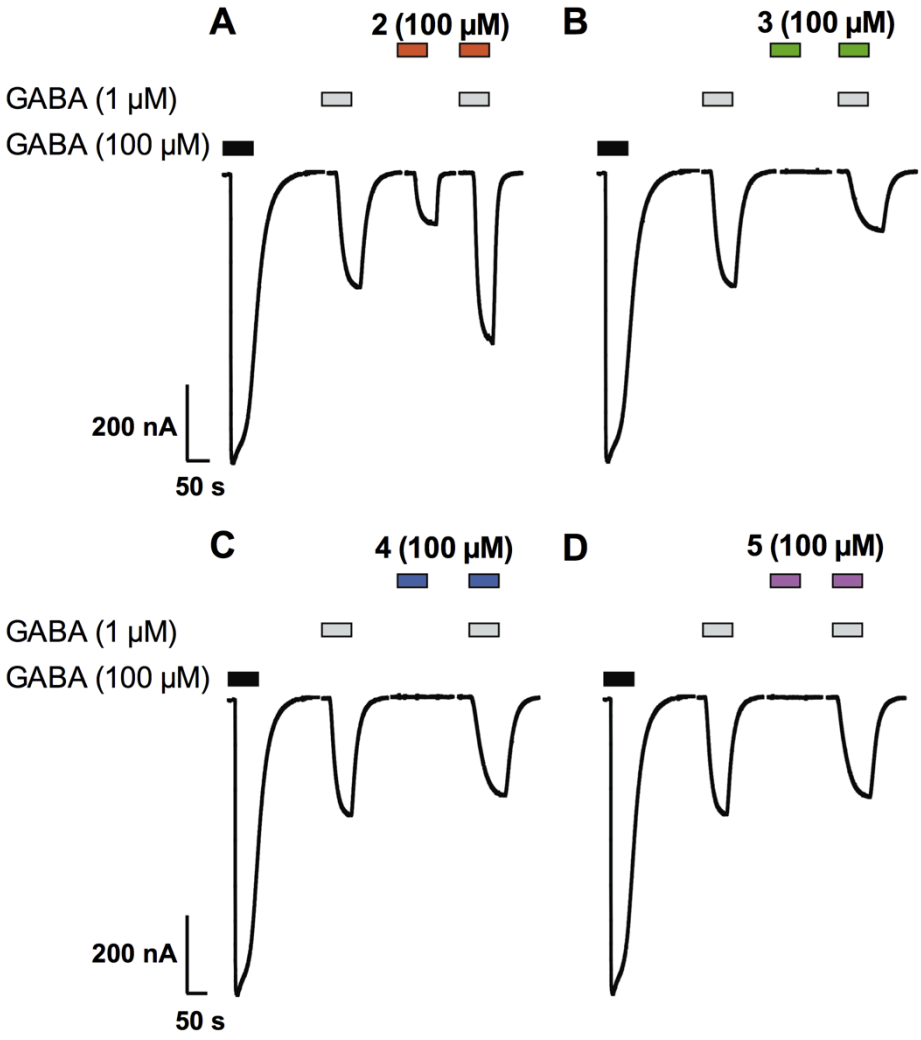

The Figure above contains sample current traces (nA vs sec) showing the effect of **2**–**5** on ρ1 receptors ($GABA_c$) in *Xenopus* oocytes. **A**. Sample current trace showing weak agonist effect of **2** at 100 μM (red bar). **2** had additive effects in the presence of GABA (1 μM) (grey bar) indicating no antagonist properties. **B**. **3** had no agonist effect at 100 μM (green bar) but inhibited the current produced by GABA (1 μM) (grey bar) by 50.2 %. **C**. **4** had no agonist effect at 100 μM (blue bar). However the current produced by GABA (1 μM) (grey bar) was inhibited by 14.8 % in the presence of **5** (100 μM) (purple bar). **D**. **5** had no agonist effect at 100 μM (purple bar). However the current produced by GABA (1 μM) (grey bar) was inhibited by 15.4 % in the presence of **5** (100 μM) (purple bar).

Homology modeling and docking studies

Homology model of ρ1 GABAC was generated by using the 'prime' suite in Maestro.[15] The crystal structure of the acetylcholine binding protein[16] (AChBP) from *L. stagnalis* (PDB code: 1I9B) was used as a template for generating the model. The sequence of ρ1 GABAC (accession code: P24046) was aligned on the template in similar way to that of Adamian and Abdel-Halim *et al*.[17,18] Five subunits of the ρ1 GABAC were individually made and merged to form a ρ1 GABAC homopentmaric model. The OPLS_2005 all-atom force field was used for energy scoring of the protein and surface generalized Born (SGB) continuum solvation model for treating solvation energies and effects. The predicted model was then prepared for docking by using protein preparation wizard, wherein hydrogens were added, bond orders assigned and disulphide bonds created. Finally the corrected structure was optimized by restrained minimization using "impref minimization" by selecting hydrogens only so that heavy atoms were left untouched. Docking studies were conducted using "Glide" software as provided in Maestro.[19] A docking model was generated by forming a receptor grid around the active site amino acids of the two adjacent $GABA_C$ monomers. The centroid of Arg104, Ser168 of first chain and Tyr198 of adjacent chain was defined as the active site. The four conformers **2a**, **2b**, **3a** and **3b** were then docked into the active site using extra-precision (XP) mode.

References

1. L. Hunter, K. A. Jolliffe, M. J. T. Jordan, P. Jensen and R. B. Macquart, *Chem. Eur. J.*, 2011, **17**, 2340.
2. L. Hunter, manuscript in preparation.
3. NMR simulations were performed using the DAISY module of the Bruker TopSpin software.
4. Gaussian 09, Revision A.1, M. J. Frisch, G. W. Trucks, H. B. Schlegel, G. E. Scuseria, M. A. Robb, J. R. Cheeseman, G. Scalmani, V. Barone, B. Mennucci, G. A. Petersson, H. Nakatsuji, M. Caricato, X. Li, H. P. Hratchian, A. F. Izmaylov, J. Bloino, G. Zheng, J. L. Sonnenberg, M. Hada, M. Ehara, K. Toyota, R. Fukuda, J. Hasegawa, M. Ishida, T. Nakajima, Y. Honda, O. Kitao, H. Nakai, T. Vreven, J. A. Montgomery, Jr., J. E. Peralta, F. Ogliaro, M. Bearpark, J. J. Heyd, E. Brothers, K. N. Kudin, V. N. Staroverov, R. Kobayashi, J. Normand, K. Raghavachari, A. Rendell, J. C. Burant, S. S. Iyengar, J. Tomasi, M. Cossi, N. Rega, J. M. Millam, M. Klene, J. E. Knox, J. B. Cross, V. Bakken, C. Adamo, J. Jaramillo, R. Gomperts, R. E. Stratmann, O. Yazyev, A. J. Austin, R. Cammi, C. Pomelli, J. W. Ochterski, R. L. Martin, K. Morokuma, V. G. Zakrzewski, G. A. Voth, P. Salvador, J. J. Dannenberg, S. Dapprich, A. D. Daniels, Ö. Farkas, J. B. Foresman, J. V. Ortiz, J. Cioslowski and D. J. Fox, Gaussian, Inc., Wallingford CT, **2009**.
5. C. Lee, W. Yang and R. G. Parr, *Phys. Rev. B*, 1988, **37**, 785.
6. A. D. Becke, *J. Chem. Phys*., 1993, **98**, 5648.
7. W. J. Hehre, R. Ditchfield and J. A. Pople, *J. Chem. Phys.*, 1972, **56**, 2257.
8. P. C. Hariharan and J. A. Pople, *Theor. Chim. Acta*, 1973, **28**, 213.
9. T. Clark, J. Chandrasekhar, G. W. Spitznagel and P. v. R. Schleyer, *J. Comput. Chem.*, 1983, **4**, 294.
10. A. V. Marenich, C. J. Cramer and D. G. Truhlar, *J. Phys. Chem. B*, 2009, **113**, 6378.
11. J. Gauss, *Chem. Phys. Lett.*, 1992, **191**, 614.
12. A. Schafer, H. Horn and R. Alhrichs, *J. Chem. Phys.*, 1992, **97**, 2571.
13. T. T. Yow, E. Pera, N. Absalom, M. Heblinski, G. A. Johnston, J. R. Hanrahan and M. Chebib, *Br. J. Pharmacol.*, 2011, **163**, 1017.
14. N. Gavande, I. Yamamoto, N. K. Salam, T.-H. Ai, P. M. Burden, G. A. R. Johnston, J. R. Hanrahan and M. Chebib, *ACS Med. Chem. Lett.*, 2011, **2**, 11.
15. Prime, version 2.2, Schrödinger, LLC, New York, NY, 2009.
16. K. Brejc, W. J. van Dijk, R. V. Klaassen, M. Schuurmans, J. van der Oost, A. B. Smit and T. K. Sixma, *Nature*, 2001, **411**, 269.

17. L. Adamian, H. A. Gussin, Y. Y. Tseng, N. Muni, F. Feng, H. Qian, D. R. Pepperberg and J. Liang, *Protein Sci.*, 2009, **18**, 2371.

18. H. Abdel-Halim, J. R. Hanrahan, D. E. Hibbs, G. A. R. Johnston and M. Chebib, *Chem. Biol. Drug Des.*, 2008, **71**, 306.

19. Glide, version 5.6, Schrödinger, LLC, New York, NY, 2009.